JACS
JOURNAL OF THE AMERICAN CHEMICAL SOCIETY

ARTICLE

pubs.acs.org/JACS

Synthesis and Characterization of a Series of Highly Fluorogenic Substrates for Glutathione Transferases, a General Strategy

Jie Zhang,[†] Aya Shibata,[‡] Mika Ito,[‡,§] Satoshi Shuto,[§] Yoshihiro Ito,[‡] Bengt Mannervik,[∥,⊥] Hiroshi Abe,[*,‡] and Ralf Morgenstern[*,†]

[†]Institute of Environmental Medicine, Division of Biochemical Toxicology, Karolinska Institutet, SE 17177 Stockholm, Sweden
[‡]Nano Medical Engineering Laboratory, RIKEN Advanced Science Institute, 2-1 Hirosawa, Wako-Shi, Saitama 351-0198, Japan
[§]Faculty of Pharmaceutical Sciences, Hokkaido University, Kita-12, Nishi-6, Kita-ku, Sapporo 060-0812, Japan
[∥]Department of Biochemistry, Uppsala University, Biomedical Center, Box 576, SE-751 23 Uppsala, Sweden
[⊥]Department of Neurochemistry, Stockholm University, SE-10691 Stockholm, Sweden

Supporting Information

ABSTRACT:

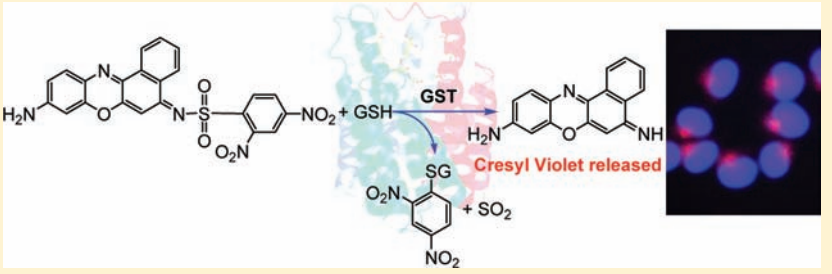

Glutathione transferases (GSTs) are used in biotechnology applications as fusion partners for facile purification and are also overexpressed in certain tumors. Consequently, there is a need for sensitive detection of the enzymes. Here we describe a general strategy for the synthesis and characterization of novel fluorogenic substrates for GSTs. The substrates were synthesized by introducing an electrophilic sulfonamide linkage to fluorescent molecules containing an amino group [e.g., 2,4-dinitrobenzenesulfonamide (DNs) derivatives of coumarin, cresyl violet, and rhodamine]. The derivatives were essentially nonfluorescent, and upon GST catalyzed cleavage of the dinitrobenzenesulfonamide, free fluorophore is released (and 1-glutathionyl-2,4-dinitrobenzene + SO_2). All the coumarin-, cresyl violet- and rhodamine-based fluorogenic probes turned out to be good substrates for most GSTs, especially for $GSTA_{1-1}$, in terms of strong fluorescence increases (71−1200-fold), high k_{cat}/K_m values (10^4−10^7 M^{-1} s^{-1}) and significant rate enhancements (10^6−10^9-fold). The substrates were successfully applied to quantitate very low levels of GST activity in cell extracts and DNs-cresyl violet was also successfully applied to the imaging of microsomal $MGST_1$ activity in living cells. The cresyl violet stained cells retained their fluorescence after fixation, which is a very useful property. In summary, we describe a general and versatile strategy to generate fluorogenic GST substrates, some of them providing the most sensitive assays so far described for GSTs.

INTRODUCTION

Fluorogenic substrates are crucial to develop sensitive biotechnology applications (e.g., screening/reporter assays), single molecule enzymology, and specific cell and tissue staining. A method that allows the conversion of existing ultrabright fluorophores to highly fluorogenic, essentially nonfluorescent, enzyme substrates is therefore of strong interest. Here we describe a general strategy that converts free amino group containing fluorophores to glutathione transferase (GST) substrates. The GSTs are remarkably indiscriminate, allowing a variety of fluorophore structures. As glutathione transferases are overexpressed in many tumors and used as biotechnological tools (easily purified fusion partners), this strategy should be of general use.

Glutathione transferases (GSTs, EC 2.5.1.18) are phase II detoxification enzymes that catalyze the basic reaction in which glutathione (GSH) is added to an electrophilic center of a hydrophobic compound that can be of both endogenous and exogenous origin.[1] In addition to the GSH conjugation activity, these enzymes also carry out a wide range of other functions, including glutathione peroxidase (GPx) and isomerase activity, biosynthesis of steroid hormones and prostaglandins, and modulation of signaling pathways.[2] GSTs play an important role in cellular protection from environmental and oxidative stress yet are also implicated in cellular resistance to drugs.[3−5] Mammalian GSTs are divided into three main families: cytosolic, mitochondrial, and membrane-bound microsomal. The cytosolic family is further divided into seven classes: alpha, mu, omega, pi, sigma,

Received: June 22, 2011
Published: July 25, 2011

Table 1. Reported Fluorogenic Substrates as Well as the Universal Chromogenic Substrate CDNB for GSTs

		k_{cat}/K_m (M^{-1} s^{-1})				rate enhancement				
substrate	product QE	$GSTA_{1-1}$	$GSTM_{1-1}$	$GSTP_{1-1}$	$MGST_1$	$GSTA_{1-1}$	$GSTM_{1-1}$	$GSTP_{1-1}$	$MGST_1$	ref
NBD-Cl		2.7×10^6	7.6×10^4	3.1×10^5	2.6×10^5	1.3×10^7	3.8×10^5	1.6×10^6	1.3×10^6	6
SBD-Cl		3.2×10^4	3.9×10^6							7
mBCl	0.191	7.8×10^4	3.1×10^4	5.8×10^3		2.4×10^5	9.4×10^4	1.8×10^4		8, 9
Cadan		1.4×10^5	4.0×10^4	5.5×10^5	8×10^3	7.8×10^4	2.2×10^4	3.1×10^5	4.4×10^3	10
DNAF1	0.101	6.8×10^5	2.1×10^6	1.1×10^7		3.4×10^6	1.1×10^7	5.5×10^7		11
DNAF2	0.257	1.5×10^6	3.6×10^6	1.1×10^7		1.7×10^7	4.0×10^7	1.2×10^8		11
CDNB		1.4×10^4	1.4×10^4	2.2×10^4	3.3×10^5	2.0×10^6	2.0×10^6	3.1×10^6	4.8×10^7	6

theta and zeta. The microsomal GSTs are designated as "membrane-associated proteins in eicosanoid and glutathione metabolism" (MAPEG) and include microsomal GST_1 ($MGST_1$), $MGST_2$, $MGST_3$, leukotriene C_4 synthase, 5-lipoxygenase activating protein, and microsomal prostaglandin E synthase 1. MAPEG are structurally distinct from cytosolic and mitochondrial GSTs but are functionally similar in their ability to exhibit GSH conjugating and GPx activity[3,4,12] (one member, 5-lipoxygenase activating protein, is not catalytically active). Among GSTs, only $MGST_1$ is activated by sulfhydryl reagents such as *N*-ethylmaleimide (NEM) [e.g., GST activity toward 1-chloro-2,4-dinitrochlorobenzene (CDNB)[13−18] and GPx activity toward cumene hydroperoxide[19]], and the site of modification is a single cysteine residue, Cys49, within the polypeptide.[20]

So far, the measurement of GST activity has often been done with the aid of the chromogenic substrate, CDNB, which is a good substrate for many GSTs.[1] Despite its significance for detection of GST activity, its use is often limited by low sensitivity and selectivity (absorbance at 340 nm), and it should be stressed that certain forms of the enzyme (e.g., $MGST_1$[6] and GST theta[21]) display low activity with CDNB and consequently may be overlooked in samples analyzed exclusively by use of CDNB. Fluorometric detection utilizing several fluorogenic molecules has been developed for highly sensitive detection of GSH/GST activity. Representative fluorogenic reagents are 4-chloro-7-nitrobenzofurazan (NBD-Cl),[6] ammonium 4-chloro-7-sulfobenzofurazan (SBD-Cl),[7] monochlorobimane (mBCl),[8,9,22,23] 6-chloroacetyl-2-dimethylaminonaphthalene (Cadan),[10] and dinitrobenzoylaminofluorescein (DNAF)[11] (Table 1). These reagents are essentially nonfluorescent themselves and can undergo GST-catalyzed reactions to produce fluorescent GSH adducts, thus enabling highly sensitive GSH/GST activity detection. However, these probes display either high nonenzymatic reaction rates, low efficiency, narrow enzyme selectivity, low fluorescence quantum efficiency (QE), and poor stability of the GS conjugate products or have been tested only with cytosolic GSTs. Although the fluorescence off/on mechanism of the above-mentioned fluorogenic substrates differ,[11,24−27] all of them show substantial fluorescence enhancements upon GSH conjugation.

In addition to GSH conjugation activity, GSTs have been reported to exhibit sulfonamidase activity and catalyze the GSH-mediated cleavage of sulfonamide bonds to form a GS conjugate, the corresponding amine and sulfur dioxide.[28,29] Structure−activity studies with a variety of sulfonamides indicate that an electrophilic center α to the sulfonyl group is required for cleavage. On the other hand, the stability of sulfonamides is less dependent on the nature of the amine moiety.[29] These features

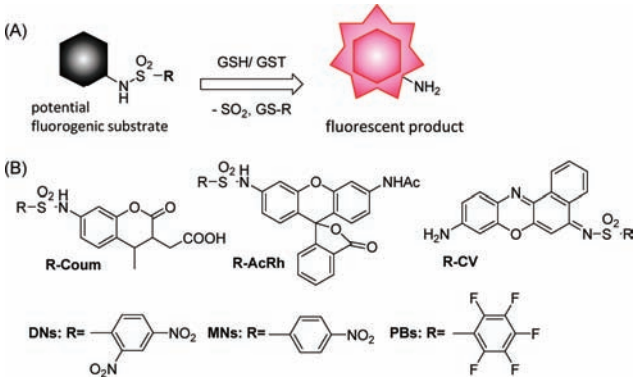

Figure 1. (A) Potential fluorogenic substrates GST-catalyzed reaction with GSH and (B) their structures.

are very advantageous and can be applied for the synthesis of sulfonamides, labile toward GSH/GST, which may serve as fluorogenic substrates to release amino-containing fluorophores. Rhodamine 110 (Rh) is highly fluorescent and resistant to photobleaching. By modifying Rh with the strongly electron withdrawing 2,4-dinitrobenzenesulfonyl (DNs) group, the molecule becomes essentially nonfluorescent, and the resulting fluorogenic bis-2,4-dinitrobenzenesulfonyl rhodamine (bis-DNs-Rh) has been used for the detection of biological thiols as well as thiols in HeLa cells.[30] Previous studies in our laboratory showed that the electrophilic center α to the DNs group is attacked by GSH and that this reaction is catalyzed by both cytosolic and membrane-bound GSTs releasing the free Rh dye.[31] These results were quite promising and suggested that any amino-containing fluorophore could be derivatized in a similar way and serve as a potential GST substrate. This design strategy is straightforward and versatile and can provide significantly greater sensitivity, compared to methods where the fluorophore produces a GS conjugate. To demonstrate the working hypothesis, synthesis of different fluorogenic probes for GSTs was carried out, including that of 7-dinitrobenzenesulfonamino-4-methyl-3-coumarinylacetic acid (DNs-Coum), DNs-*N*-acetylrhodamine (DNs-AcRh), and DNs-cresyl violet (DNs-CV). Compared to bis-DNs-Rh, DNs-AcRh contains only a single hydrolysis-sensitive sulfonamide moiety, thus avoiding the complicated biphasic kinetics of disubstituted Rh-based substrates. In order to examine the influence of chemical reactivity on enzyme activity and background rates, para-substituted 4-mononitrobenzenesofonyl (MNs), 4-toluenesulfonyl (Ts), and pentafluorobenzenesulfonyl (PBs) derivatives were synthesized as well. The potential substrates and their reaction with GSH are depicted in Figure 1. Fluorescence emissions of the products shift gradually to

Table 2. Quantum Efficiencies of the Compounds[a]

fluorogenic substrate	QE	product	QE	fluorescence activation fold
DNs-Coum	0.009	Coum	0.641	71
DNs-AcRh	0.0036	AcRh	0.387	110
MNs-AcRh	0.0059			66
PBs-AcRh	0.0256			15
DNs-CV	0.0004	CV	0.23	580
MNs-CV	0.0002			1200

[a] DNs-Coum and Coum measurements were done in sodium phosphate buffer (100 mM, pH 10). Compounds were excited at 375 nm. Quantum yields are determined by using 4-methylumbelliferone (0.63, 0.1 M phosphate buffer (pH 10) as a standard. DNs-AcRh, MNs-AcRh, PBs-AcRh, and AcRh measurements were done in sodium phosphate buffer (100 mM, pH 7.4). Compounds were excited at 490 nm. Quantum yields are determined by using fluorescein (0.85, 0.1 M NaOH) as standard. DNs-CV, MNs-CV, and CV measurements were done in sodium phosphate buffer (100 mM, pH 7.4). Compounds were excited at 540 nm. Quantum yields are determined by using CV (0.54, MeOH) as standard.

longer wavelengths, from 450 to 620 nm. Therefore, this series of probes can offer multiple color detection in living cells and other biological matrices, giving blue, green and red color under fluorescence microscopy. An important application of our fluorogenic GST substrates could be in imaging of cancer cells that overexpress GSTs. However, this implies broad isoenzyme substrate selectivity.

Here we present, for the first time, a general strategy to produce fluorogenic substrates for both cytosolic and membrane-bound GSTs. First of all, specific activities were determined for a panel of recombinant cytosolic GSTs and purified $MGST_1$. High activities were obtained with DNs-Coum, DNs-AcRh and DNs-CV. Steady-state kinetic analysis of these probes was then performed with four representative enzymes, $GSTA_{1-1}$, $GSTM_{1-1}$, $GSTP_{1-1}$, and $MGST_1$. Furthermore, DNs-Coum, DNs-AcRh, and DNs-CV were highly sensitive and useful to quantitate GST activity in cell extracts, and DNs-CV was successfully applied to the imaging of $MGST_1$ activity in living cells.

RESULTS

Synthesis of the Fluorogenic Probes. The synthesis of DNs-Coum was described in our previous paper.[32] DNs-AcRh, MNs-AcRh, and PBs-AcRh were synthesized according to Scheme S1 (Supporting Information). The amino group of mono-Boc-rhodamine 110[33] was protected by an acetyl group. And then, the Boc group was removed by treatment with 4 M HCl/dioxane solution to give the AcRh. The desired products, benzene sulfonamide-protected rhodamine derivatives (DNs-AcRh, MNs-AcRh and PBs-AcRh), were obtained by treatment of AcRh with DNs-Cl, MNs-Cl, or PBs-Cl in pyridine/CH_2Cl_2 for 5−16 h in 37%, 42%, or 47% yield, respectively. The synthesis of DNs-CV, MNs-CV, and Ts-CV was carried out according to Scheme S2 (Supporting Information). The treatment of CV with DNs-Cl, MNs-Cl, or Ts-Cl under various basic conditions successfully gave the desired products, DNs-CV (30%), MNs-CV (69%), or Ts-CV (47%).

Characterization of the Fluorogenic Probes. Generally, development of fluorogenic substrates for enzyme assays faces two main difficulties. One is to achieve fluorescence activation by a specific reaction, and the other is to ensure that the target enzyme recognizes the compound as a specific substrate.[11] To fulfill these two prerequisites, we first measured the fluorescence quantum efficiencies of the fluorogenic probes and their fluorophore metabolites. As shown in Table 2, the fluorogenic probes, DNs-Coum, DNs-AcRh, MNs-AcRh, PBs-AcRh, DNs-CV, and MNs-CV, show very low fluorescence quantum efficiencies, in contrast to the high efficiencies of Coum, AcRh, and CV. This result is ideal in terms of fluorescence activation. Next, we needed to find out whether these sulfonamides can be readily cleaved by the GS^- thiolate and whether these reactions are specifically catalyzed by GSTs. The probes were incubated in solution with or without GSH/GST, and the resulting absorption and fluorescence spectra are shown in Figures 2 and 3, respectively. The DNs-Coum and Coum showed a maximum absorption at 342 and 341 nm, respectively, in 10 mM PBS (pH 7.4) (Figure 2A). A decrease in the absorption of DNs-AcRh at 490 nm was observed compared with AcRh due to the formation of lactone ring (Figure 2B). The DNs-CV and CV showed a maximum absorption at 607 and 594 nm, where lower absorption was observed in DNs-CV (Figure 2C). Without GSH/GST, no significant fluorescence was observed from the fluorogenic probes (Figure 3). After the addition of GSH to the solution of fluorogenic probes, a low emission appeared around 450, 520, and 620 nm, respectively. On the other hand, with GSH/GST, a strong emission appeared and the emission was enhanced 62−290-fold. The results demonstrated that all probes are potentially good fluorogenic substrates for GSTs. Therefore, in the next round of experiments, specific activities of both cytosolic and membrane-bound GSTs toward these probes, as well as steady-state kinetic characteristics, were carefully examined.

GST Activity toward Fluorogenic Probes. Specific activities were determined for cytosolic GSTs, $GSTA_{1-1}$, $GSTA_{2-2}$, $GSTA_{3-3}$, $GSTA_{4-4}$, $GSTM_{1-1}$, $GSTM_{2-2}$, $GSTP_{1-1}$, and $GSTT_{1-1}$, as well as membrane-bound $MGST_1$, using DNs-Coum, DNs-AcRh, MNs-AcRh, PBs-AcRh, DNs-CV, MNs-CV, and Ts-CV (Table 3). In general, all of the probes, except MNs-CV and Ts-CV, are good substrates for all GSTs, except for $GSTT_{1-1}$. The highest activities were found with DNs-AcRh, DNs-Coum, and DNs-CV, and the activities for $GSTA_{1-1}$ with these probes were more than 2-fold higher than for other GSTs. With DNs-Coum and DNs-AcRh, $MGST_1$ showed much lower activity compared with cytosolic GSTs (except $GSTT_{1-1}$). In contrast, with DNs-CV, the activities of $MGST_1$ were higher or comparable with those of cytosolic GSTs (except $GSTA_{1-1}$).

When the DNs group was replaced by a MNs group, a dramatic decrease (more than 1000-fold) was observed in activity for all GSTs, presumably due to the low reactivity. In this case, the activities for $GSTM_{1-1}$ and $GSTM_{2-2}$ with MNs-AcRh and MNs-CV were higher than for other GSTs. The replacement of DNs group with a Ts group resulted in loss of activity for all GSTs. When the DNs group was replaced by PBs group, the activities were more than 100-fold lower for all GSTs. The activity for $GSTP_{1-1}$ with PBs-AcRh was higher than for other GSTs. Thus, manipulating substrate reactivity alters enzyme selectivity.

Steady-State Kinetics with Selected Fluorogenic Probes. In order to gain deeper insight into the rate behavior toward different fluorogenic probes, a steady-state kinetic analysis of DNs-Coum, DNs-AcRh, MNs-AcRh, PBs-AcRh, and DNs-CV was performed with three representative cytosolic GSTs, $GSTA_{1-1}$, $GSTM_{1-1}$, and $GSTP_{1-1}$, and membrane-bound $MGST_1$. To determine whether a highly efficient fluorogenic

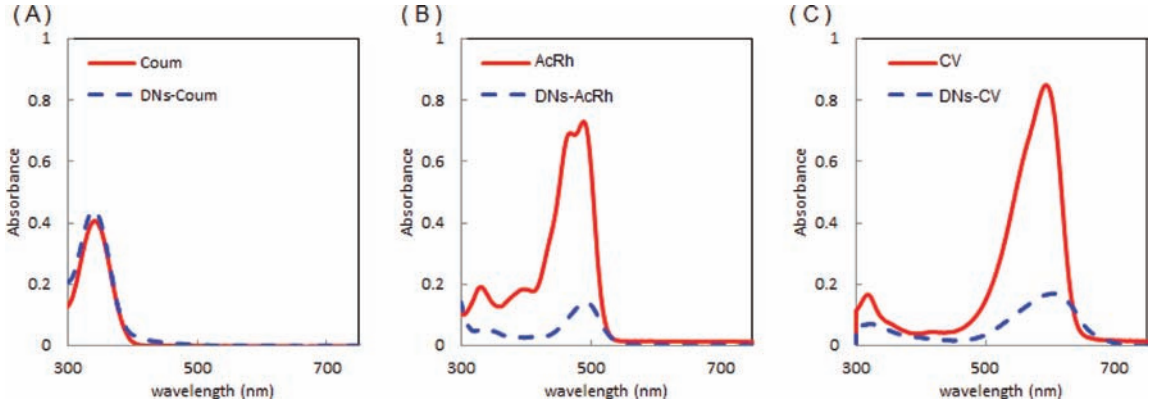

Figure 2. Absorption spectra of 20 μM fluorogenic probes and 20 μM products in 10 mM PBS (pH7.4). (A) DNs-Coum and Coum, (B) DNs-AcRh and AcRh, and (C) DNs-CV and CV. Absorption spectra were observed by UV/vis spectrophotometer (V-550, JASCO).

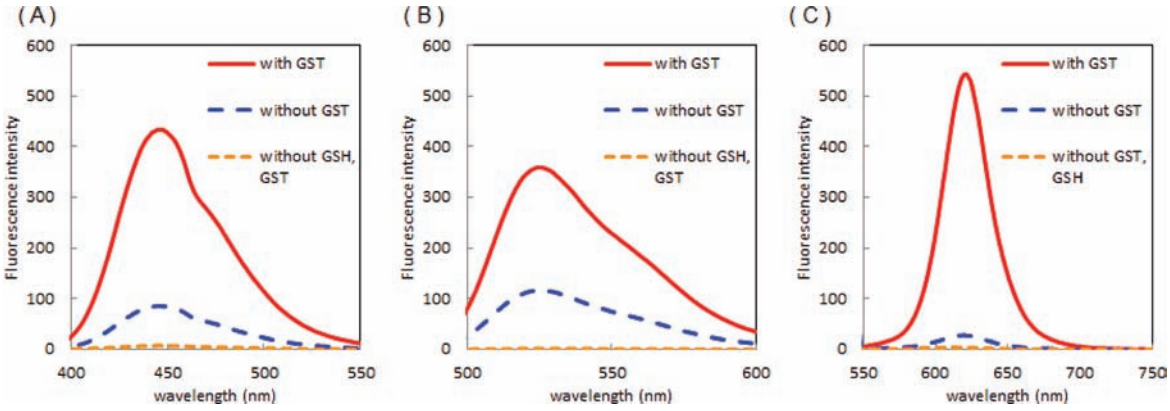

Figure 3. Fluorescence measurement of the fluorogenic probes in the absence or presence of GSH/GST. Reactions were performed in 10 mM PBS (pH7.4) with 1 μM probe, 10 mM GSH, and 2 μg/mL GST for 8 min at 37 °C. Fluorescence spectra were observed by fluorescence spectrophotometry (FP-6500, JASCO). The fluorescence with excitation of (A, DNs-Coum) 345 nm was obtained a scan range of 400−550 nm, (B, DNs-AcRh) 490 nm was obtained a scan range of 500−600 nm, and (C, DNs-CV) 540 nm was obtained a scan range of 500−750 nm.

Table 3. Specific Activity of GSTs with Different Fluorogenic Substrates[a]

	specific activity (nmol min^{-1} mg^{-1})								
substrate	$GSTA_{1-1}$	$GSTA_{2-2}$	$GSTA_{3-3}$	$GSTA_{4-4}$	$GSTM_{1-1}$	$GSTM_{2-2}$	$GSTP_{1-1}$	$GSTT_{1-1}$	$MGST_1$
DNs-Coum	1700 ± 160	230 ± 30	660 ± 210	370 ± 60	810 ± 110	330 ± 40	690 ± 60	ND	130 ± 2
DNs-AcRh	6700 ± 200	490 ± 30	930 ± 100	520 ± 100	2700 ± 200	990 ± 90	2300 ± 560	0.28 ± 0.04	420 ± 60
MNs-AcRh	0.23 ± 0.4	0.18 ± 0.01	0.24 ± 0.1	0.13 ± 0.04	0.31 ± 0.02	0.31 ± 0.06	0.22 ± 0.01	ND	0.0011 ± 0.0001
PBs-AcRh	6.7 ± 0.3	0.15 ± 0.01	3.1 ± 0.4	0.47 ± 0.04	0.94 ± 0.09	0.45 ± 0.06	9.0 ± 0.6	0.0016 ± 0.0001	0.50 ± 0.06
DNs-CV	1500 ± 100	150 ± 20	480 ± 90	770 ± 210	550 ± 100	410 ± 50	460 ± 50	0.062 ± 0.007	560 ± 80
MNs-CV	ND	ND	ND	ND	0.085 ± 0.013	0.038 ± 0.021	ND	ND	ND
Ts-CV	ND	ND	ND	ND	ND	ND	ND	ND	ND

[a] Specific activities were obtained in 0.1 M potassium phosphate buffer pH 6.5 (with 0.1% Triton for $MGST_1$), 5 mM GSH, and DNs-Coum, DNs-AcRh, MNs-AcRh, PBs-AcRh, DNs-CV, MNs-CV, or Ts-CV as second substrate. The concentration of DNs-Coum used was 40 μM, the concentration of DNs-AcRh, MNs-AcRh, and PBs-AcRh used was 25 μM, and the concentration of DNs-CV, MNs-CV, and Ts-CV used was 2.5 μM. The final DMSO concentration in all assays was 1.0% (v/v). ND, not detectable. Values are means ± standard deviations (n = 3).

substrate has been found, the most useful catalytic constant is k_{cat}/K_m, sometimes called the specificity constant, representing the apparent second-order rate constant for the association of substrate and free enzyme to form product and free enzyme. There is an upper limit to k_{cat}/K_m, imposed by diffusion, i.e., the rate at which enzyme and substrate collide in aqueous solution. The diffusion-controlled limit is 10^8-10^9 M^{-1} s^{-1}. Enzymes having a k_{cat}/K_m near this range are said to have achieved catalytic perfection.[34,35] k_{cat}/K_m values of GSTs with different fluorogenic probes are shown in Figure 4. $GSTA_{1-1}$ is the most efficient enzyme for all the DNs-derivatized fluorogenic substrates (DNs-Coum, DNs-CV, and DNs-AcRh), with k_{cat}/K_m values

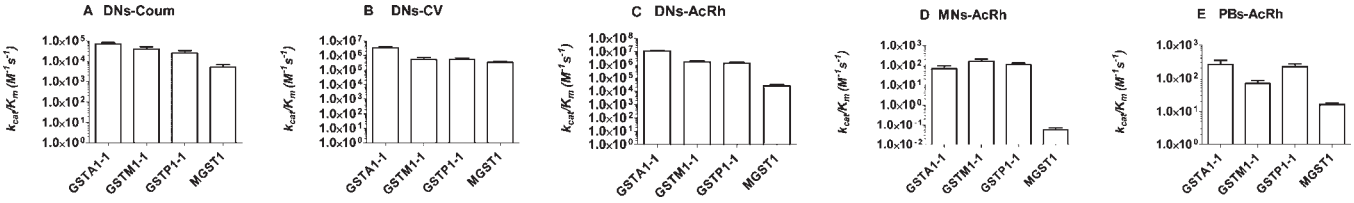

Figure 4. Catalytic efficiencies of GSTs with different fluorogenic substrates. The catalytic efficiencies (k_{cat}/K_m) of $GSTA_{1-1}$, $GSTM_{1-1}$, $GSTP_{1-1}$, and $MGST_1$ were determined with (A) DNs-Coum, (B) DNs-CV, (C) DNs-AcRh, (D) MNs-AcRh, and (E) PBs-AcRh. Values are means ± standard errors of the mean ($n \geq 6$).

Table 4. Steady-State Kinetic Parameters of GST with Alternative Fluorogenic Substrates[a]

substrate	parameters	$GSTA_{1-1}$	$GSTM_{1-1}$	$GSTP_{1-1}$	$MGST_1$
DNs-Coum	K_m (μM)	14 ± 2	12 ± 3	17 ± 5	47 ± 12
	k_{cat} (s^{-1})	1.0 ± 0.1	0.47 ± 0.05	0.43 ± 0.06	0.24 ± 0.03
	k_{cat}/K_m (M^{-1} s^{-1})	(7.1 ± 1.2) × 10^4	(3.9 ± 1.1) × 10^4	(2.5 ± 0.8) × 10^4	(5.1 ± 1.5) × 10^3
DNs-CV	K_m (μM)	0.18 ± 0.03	0.45 ± 0.15	0.49 ± 0.13	4.5 ± 0.7
	k_{cat} (s^{-1})	0.60 ± 0.03	0.23 ± 0.02	0.25 ± 0.02	1.5 ± 0.1
	k_{cat}/K_m (M^{-1} s^{-1})	(3.3 ± 0.8) × 10^6	(5.1 ± 2.0) × 10^5	(5.1 ± 1.4) × 10^5	(3.3 ± 0.6) × 10^5
DNs-AcRh	K_m (μM)	0.29 ± 0.02	0.72 ± 0.12	0.87 ± 0.18	38 ± 8
	k_{cat} (s^{-1})	3.1 ± 0.1	1.2 ± 0.1	1.1 ± 0.1	1.0 ± 0.1
	k_{cat}/K_m (M^{-1} s^{-1})	(1.1 ± 0.1) × 10^7	(1.7 ± 0.3) × 10^6	(1.3 ± 0.3) × 10^6	(2.6 ± 0.6) × 10^4
MNs-AcRh	K_m (μM)	1.5 ± 0.2	0.87 ± 0.11	0.99 ± 0.19	>25[b]
	k_{cat} (s^{-1})	(1.0 ± 0.4) × 10^{-4}	(1.4 ± 0.4) × 10^{-4}	(1.1 ± 0.1) × 10^{-4}	ND[c]
	k_{cat}/K_m (M^{-1} s^{-1})	67 ± 28	160 ± 50	110 ± 20	0.056 ± 0.009[d]
PBs-AcRh	K_m (μM)	17 ± 5	6.8 ± 1.5	41 ± 8[e]	>200[f]
	k_{cat} (s^{-1})	(4.4 ± 0.6) × 10^{-3}	(4.7 ± 0.4) × 10^{-4}	(9.1 ± 1.0) × 10^{-3}	ND[c]
	k_{cat}/K_m (M^{-1} s^{-1})	260 ± 80	69 ± 16	220 ± 50	16 ± 1[d]

[a] The cytosolic GST ($GSTA_{1-1}$, $GSTM_{1-1}$, or $GSTP_{1-1}$) was assayed in 0.1 M potassium phosphate buffer pH 6.5, at a constant GSH concentration of 5 mM and varying concentrations of DNs-Coum (1.25−40 μM), DNs-CV (0.1−2.5 μM), DNs-AcRh (0.049−6.25 μM), MNs-AcRh (0.39−25 μM), or PBs-AcRh (0.78−50 μM), whereas $MGST_1$ was assayed in 0.1 M potassium phosphate buffer pH 6.5 with 0.1% Triton, at a constant GSH concentration of 5 mM and varying concentrations of DNs-Coum (2.5−80 μM), DNs-CV (0.63−20 μM), DNs-AcRh (1.56−100 μM), MNs-AcRh (12.5 and 25 μM), or PBs-AcRh (25−200 μM). The final concentration of the solvent DMSO was <1% unless otherwise specified. Error limits are given by Graphpad Prism 5 after fitting by nonlinear regression; in general, at least 18 observations were included in the data sets. [b] The hydrophobic nature of MNs-AcRh makes it difficult to obtain saturation kinetics. The highest concentration used was 25 μM. [c] ND, not determined. [d] The apparent k_{cat}/K_m value was obtained using the Michaelis−Menten relationship at low substrate concentration: $v/[E][S] = k_{cat}/K_m$, when $[S] < K_m$. Values are means ± standard errors of the mean ($n \geq 6$). [e] The enhanced inner-filter effect at high concentrations of PBs-AcRh makes it difficult to obtain saturation kinetics. The highest concentration used was 50 μM. [f] The enhanced DMSO concentration (the concentration of the PBs-AcRh stock solution was 10 mM in DMSO) at high concentrations of PBs-AcRh makes it difficult to obtain saturation kinetics. The highest concentration used was 200 μM (2% DMSO as cosolvent).

approaching 10^5, 10^7, and 10^8, respectively. For DNs-Coum and DNs-AcRh, $MGST_1$ showed much lower efficiencies compared with all cytosolic GSTs. Whereas for DNs-CV, the efficiencies of $MGST_1$ were comparable with those of $GSTM_{1-1}$ and $GSTP_{1-1}$, with k_{cat}/K_m values approaching 10^6.

The effect of the substituent in the aromatic ring, α to the sulfonyl group, on the catalytic efficiency was investigated with the Rh-based fluorogenic substrates (DNs-AcRh, MNs-AcRh, and PBs-AcRh). The catalytic efficiencies with DNs-AcRh as a substrate were generally 4 orders of magnitude greater than those with MNs-AcRh and 3 orders of magnitude greater than those with PBs-AcRh. For DNs-AcRh and PBs-AcRh, $GSTA_{1-1}$ showed higher efficiencies compared with other GSTs, whereas for MNs-AcRh, the k_{cat}/K_m value for $GSTM_{1-1}$ was higher than for other GSTs (Figure 4C−E).

k_{cat} and K_m values are summarized in Table 4. k_{cat} values are in the 1 s^{-1} range, and the high catalytic efficiencies are depending

Table 5. Second-Order Rate Constant for the Nonenzymatic Reaction[a]

	k_{noncat} (M^{-1} s^{-1})	
substrate	without 0.1% Triton X-100	with 0.1% Triton X-100
DNs-Coum	0.017 ± 0.001	0.016 ± 0.001
DNs-CV	(1.4 ± 0.3) × 10^{-3}	(7.7 ± 0.8) × 10^{-4}
DNs-AcRh	0.16 ± 0.01	(1.4 ± 0.1) × 10^{-3}
MNs-AcRh	(4.9 ± 0.3) × 10^{-6}	ND[b]
PBs-AcRh	(1.5 ± 0.1) × 10^{-5}	(1.4 ± 0.1) × 10^{-5}

[a] The second-order rate constant for the nonenzymatic reaction (k_{noncat}) was obtained in 0.1 M potassium phosphate buffer pH 6.5 (without or with 0.1% Triton), at a constant GSH concentration of 5 mM and varying concentrations of DNs-Coum, DNs-CV, DNs-AcRh, MNs-AcRh, or PBs-AcRh, same as mentioned in Table 4. [b] ND, not detectable. Values are means ± standard errors of the mean ($n \geq 6$).

Table 6. Rate Enhancements Produced by GSTs[a]

	$GSTA_{1-1}$	$GSTM_{1-1}$	$GSTP_{1-1}$	$MGST_1$
DNs-Coum	$(4.1 \pm 0.7) \times 10^6$	$(2.3 \pm 0.6) \times 10^6$	$(1.5 \pm 0.5) \times 10^6$	$(3.2 \pm 0.9) \times 10^5$
DNs-CV	$(2.4 \pm 1.1) \times 10^9$	$(3.6 \pm 2.1) \times 10^8$	$(3.6 \pm 2.1) \times 10^8$	$(4.3 \pm 1.2) \times 10^8$
DNs-AcRh	$(6.8 \pm 0.6) \times 10^7$	$(1.1 \pm 0.2) \times 10^7$	$(8.0 \pm 1.8) \times 10^6$	$(1.9 \pm 0.4) \times 10^7$
MNs-AcRh	$(1.4 \pm 0.6) \times 10^7$	$(3.3 \pm 1.1) \times 10^7$	$(2.3 \pm 0.5) \times 10^7$	ND
PBs-AcRh	$(1.7 \pm 0.6) \times 10^7$	$(4.5 \pm 1.2) \times 10^6$	$(1.4 \pm 0.4) \times 10^7$	$(1.1 \pm 0.2) \times 10^6$

[a] For assay conditions, see Tables 4 and 5. Values are means ± standard errors of the mean ($n \geq 6$).

on low K_m values. The low K_m values for the DNs derivatives are most likely due to the high reactivity of the compounds, as the less reactive analogues MNs and PBs display considerably higher K_m values. This rate behavior precludes the simplest Michaelis–Menten mechanism, where K_m is a combination of substrate release/binding and chemical conversion $(k_{-1} + k_2)/k_1$, consistent with earlier kinetic characterization of these enzymes.[36]

In conclusion, so far, all the DNs-derivatized fluorogenic substrates (DNs-AcRh, DNs-Coum, and DNs-CV) are good substrates for most GSTs, except $GSTT_{1-1}$. The broad enzyme specificity, high catalytic efficiencies, and the highly sensitive fluorescence-based assay enable these fluorogenic substrates to be attractive alternatives to the universal chromogenic substrate CDNB for GST activity measurement. The nature of the electrophilic group in the sulfonyl moiety markedly affects the enzyme reactivity and selectivity. A strong electrophilic center α to the sulfonyl group is required for high GSH/GST activity. Replacement of the ortho- and para-dinitro (DNs) group with para-mononitro (MNs) or PBs group results in a dramatic decrease in both activity and catalytic efficiency for all GSTs, and the replacement with a para-methyl (Ts) group resulted in loss of activity. The DNs-derivatized fluorogenic substrates display selectivity for $GSTA_{1-1}$, whereas the MNs-derivatized fluorogenic substrates display selectivity for $GSTM_{1-1}$ and $GSTM_{2-2}$, and the PBs-derivatized fluorogenic substrates display selectivity for $GSTA_{1-1}$ and $GSTP_{1-1}$. The nature of the amine moiety (fluorophore) influences the enzyme reactivity and selectivity as well, though the differences are not remarkable. For cytosolic GSTs, the activities and catalytic efficiencies with DNs-Rh were mostly higher than those with DNs-Coum and DNs-CV, whereas membrane-bound $MGST_1$ showed higher activity and catalytic efficiency with DNs-CV.

In order to assess the rate enhancement, the second-order rate constant of the nonenzymatic reaction, k_{noncat}, was determined to compare with the apparent second-order rate constant for the enzyme-catalyzed reaction, k_{cat}/K_m. Since the enzymatic reaction was performed both with and without 0.1% Triton X-100, the same assay conditions were applied to determine k_{noncat}, and the results are summarized in Table 5. The chemical properties of the different derivatives are clearly reflected in k_{noncat} in a logical fashion, as the reactivity of the aromatic substituent is decreased (DNs-AcRh to PBs-AcRh and MNs-AcRh). Interestingly, the fluorogenic moiety has a 2 orders of magnitude influence on the background rate, with DNs-CV showing a very low value. In the presence of detergent, the more hydrophobic fluorogenic molecules display much lower rates, as they are probably shielded from reaction with the hydrophilic GSH by partitioning into the detergent micelles. The observed trend in nonenzymatic reactivity is reflected also in the k_{cat}/K_m values (Figure 4), resulting in quite similar rate enhancement for DNs-AcRh, MNs-AcRh, and PBs-AcRh (Table 6). Overall the cresyl violet derivative displays superior rate enhancement with all enzymes tested.

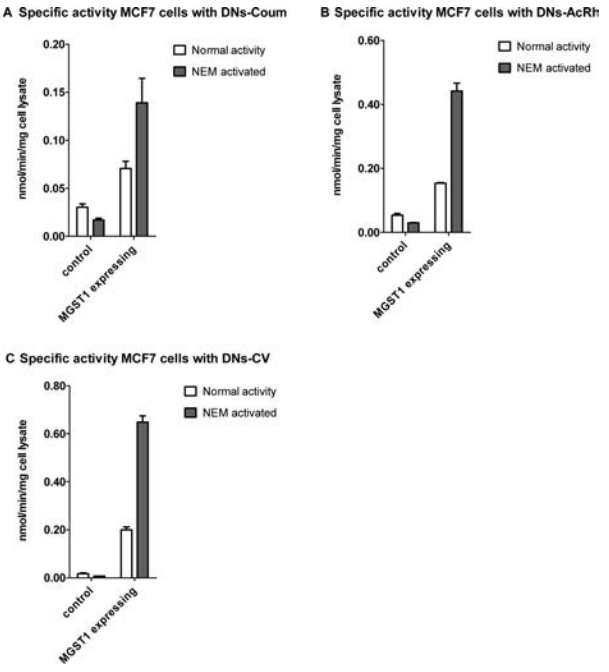

Figure 5. Specific activity of GST in cell lysate with fluorogenic substrate: (A) 40 μM DNs-Coum, (B) 25 μM DNs-AcRh, and (C) 2.5 μM DNs-CV. Values are means ± standard errors of the mean ($n \geq 3$).

GST Activity in MCF_7 Cell Lysates. It is often desirable to be able to detect very low levels of enzymatic activities in cell extracts, tissues, or clinical specimens. Therefore, we tested whether DNs-Coum, DNs-AcRh, and DNs-CV could measure the GST activity in MCF_7 cell lysates and whether the differences of GST activity in $MGST_1$-expressing and vector control MCF_7 cells could be detected by these fluorogenic substrates. Human MCF_7 breast cancer cells have very low GST activity and have often been used for transfection experiments with GSTs.[37−40] For all fluorogenic substrates tested, extracts from $MGST_1$-expressing MCF_7 cells were more efficient at catalyzing the reaction compared with the vector control cells (under normal conditions and after NEM preincubation to activate $MGST_1$). The most significant differences in specific activity between $MGST_1$-expressing cells and vector control cells were found with DNs-CV, consistent with DNs-CV being the best substrate for $MGST_1$ (Figure 5). The activity could be increased in $MGST_1$-expressing cell extracts by NEM preincubation as expected, whereas the activity in the vector control cells was decreased by NEM preincubation. The low (and NEM sensitive) activity in vector control cells most likely stems from the low

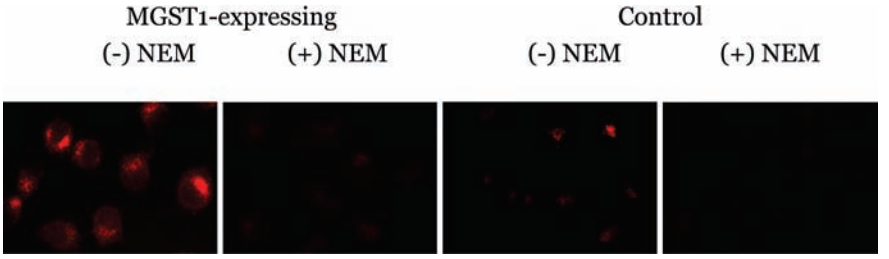

Figure 6. Fluorescence microscopic imaging of live MCF_7 cells. The $MGST_1$-expressing cells and the control cells were incubated with 2.5 μM DNs-CV for 30 min at 37 °C without or with NEM pretreatment.

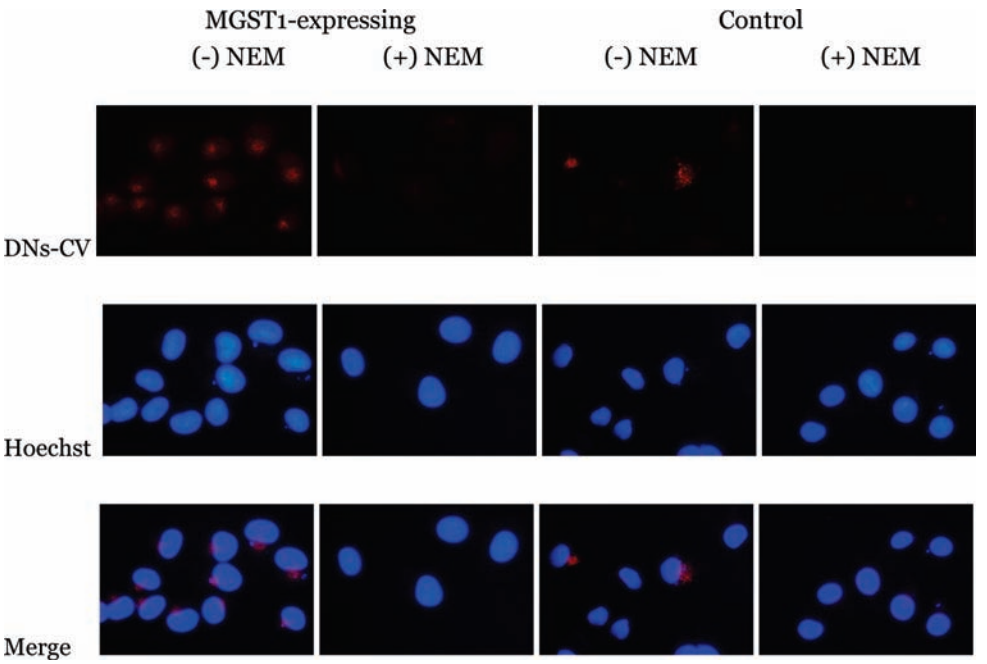

Figure 7. Fluorescence microscopic imaging of MCF_7 cells. The $MGST_1$-expressing cells and the control cells were incubated with 2.5 μM DNs-CV for 30 min at 37 °C without or with NEM pretreatment. Cells were then fixed for 15 min at room temperature with 2% formaldehyde and DNA was stained with 1 μg/mL Hoechst 33342 for 10 min at room temperature to localize nuclei.

endogenous levels of cytosolic Mu class GST, since GSTA and GSTP are essentially not expressed in MCF_7 cells.[37,39,40]

Fluorescence Microscopic Imaging of MCF_7 Cells. Since DNs-Coum, DNs-AcRh, and DNs-CV could detect differences in GST activity in cell lysates prepared from $MGST_1$-expressing cells and vector control cells, we further investigated whether the differences could be imaged by fluorescence microscopy in living cells. DNs-Coum and DNs-AcRh did not produce a marked increase of fluorescence in $MGST_1$ overexpressing or control cells. This is probably due to the higher water solubility or that their metabolites (Coum and AcRh) are easily pumped out of the cells. Incubation of cells with DNs-CV, however, resulted in a time-dependent increase in fluorescence within 30 min, as shown in Figure 6. A stronger fluorescence signal was seen in $MGST_1$-expressing cells compared with the vector control cells. Preincubation with the GSH-depleting agent, NEM, abolished the fluorescence, which confirmed that the cellular fluorescence signal can be attributed to the GSH-mediated cleavage of sulfonamide to form the corresponding fluorescent amine, cresyl violet. Cells were then stained with Hoechst 33342 to localize nuclei, and it appeared that the fluorescence signal from the released CV was localized to an area adjacent to the nucleus (Figure 7). The localization of the released dye is similar to when CV is added directly to cells and thus a property of the dye itself. After fixing the cells, the dye was still detected, which should be a quite useful property for conveniently detecting GST-expressing cells.

DISCUSSION

A General Strategy to Produce a Novel Series of Fluorogenic Substrates for GSTs. Assays wherein a fluorogenic reagent is reacted with a thiol group to form a fluorescent adduct have been known for some time. There are now many types of thiol-reactive dyes reported for GSH/GST activity measurement, including benzofurazan derivatives (NBD-Cl and SBD-Cl), bimane derivatives (mBCl), naphthalene derivatives (Cadan), DNAFs, and DNAT-Me. These compounds are essentially nonfluorescent, through either intramolecular charge transfer (ICT) blocking (NBD-Cl, SBD-Cl, mBCl, and Cadan) or photon-induced electron transfer (PET) (DNAFs and DNAT-Me). The substitution of the electron-withdrawing Cl atom (NBD-Cl, SBD-Cl, mBCl, and Cadan) or nitro group (DNAFs) by the GS^- thiolate introduces an electron-donating group that

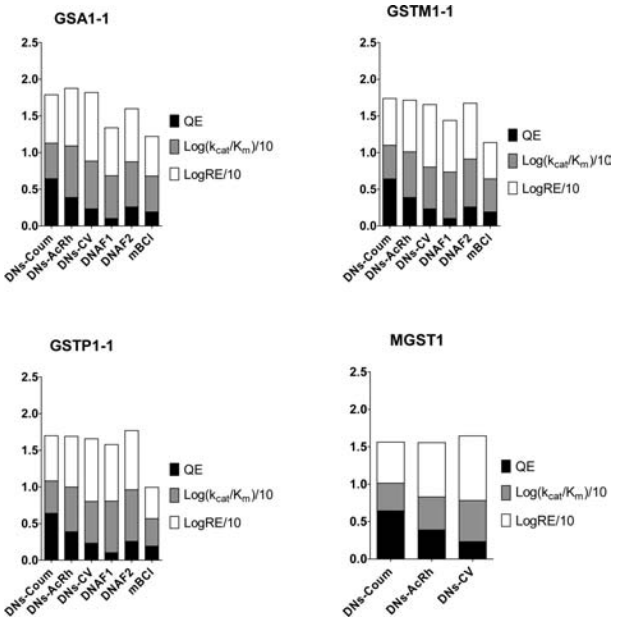

Figure 8. Comparison of different fluorogenic substrate/enzyme combinations. Quantum efficiency (QE), k_{cat}/K_m, and rate enhancements (RE) are from Tables 1, 2, 4, and 6. A perfect substrate (see the text) could in principle reach a combined score ≥2.5.

results in a dramatic increase in fluorescence. In general, for the compounds so far described, the fluorescence off/on switching happens upon glutathionylation and the fluorophore ends-up in a GS-conjugate. Many of these compounds still have drawbacks for use as a fluorogenic reagent in terms of fluorescence activation, catalytic efficiency, and rate enhancement, and therefore, there exists a need for improved fluorogenic substrates. Desirable properties are high and selective reactivity to GSH/GST, low background reaction, and highly stable fluorescent products, thereby enabling sensitive detection of very low levels of GST activity in biological samples. Here we report a general strategy to derivatize any amino group containing fluorophore and convert it to a GST substrate. This affords great versatility in terms of choosing fluorophores. So far, the different fluorescent substituents tested did not result in strong enzyme selectivity. Although it is a useful property to have broad spectrum substrates, highly selective substrates are also desirable. By altering the reactivity of the sulfonamide, very efficient substrates were created (k_{cat}/K_m up to 10^7 M^{-1} s^{-1}, Figure 4). In addition, reactivity was also coupled to changes in enzyme selectivity. Therefore, to fine-tune reactivity[36] and alter hydrophobic properties[41] opens possibilities to engineer substrate isoenzyme selectivity utilizing the electrophilic portion of the fluorogenic substrate. The rate enhancements obtained (10^5−10^9, Table 6) are equivalent to, or 2 orders of magnitude greater than, those obtained for the universal substrate CDNB (See Table 1; k_{cat}/K_m, 10^4−10^5 M^{-1} s^{-1}; rate enhancement, 10^6−$10^{7\,6}$) . If one compares specific activities toward our best fluorogenic substrates and CDNB, the latter is still around 10-fold higher with several GSTs,[1] indicating that there is room for improvement; however, as the K_m for CDNB is generally high,[6] considerably higher substrate concentrations have to be used.

Comparison to Other Fluorogenic Substrates, a General Approach. The DNs group quenches the fluorescence efficiently through different mechanisms and provides a significant fluorescent increase upon GST-catalyzed reaction with GSH (Table 2). Substituents at the C-7 position are well-known to affect the fluorescence properties of coumarins. DNs-protection quenches the emission of 7-aminocoumarins, which are highly fluorescent when deprotonated. DNs-AcRh decreased absorption at 490 nm, indicating a closed lactone form. On the other hand, AcRh in its open lactone form emits a strong fluorescence signal. In DNs-CV, the reasons for the loss of fluorescence can be attributed to the conversion of an electron-donating amine group to an electronegative sulfonamide group.[42] The most important feature of our substrates is that they are the most efficient fluorogenic GST substrates so far produced and that they generate a free (unconjugated) fluorophore. In order to facilitate the comparison of different fluorogenic substrate/enzyme combinations, we here suggest a bar graph where the most important features can be viewed in a simple fashion (Figure 8). By depicting the combination of QE (being 0−1), log k_{cat}/K_m divided by 10 (resulting in a scale that at best approaches 1), and rate enhancement (RE) (in this case using log RE divided by 10, again resulting in a scale that at best approaches 1 for the substrates/enzymes used here) in a single bar with three sections it is easy to compare quantum efficiency, catalytic efficiency, and rate enhancement (over the noncatalyzed reaction). The combined bar gives an indication of the best substrate and how far from perfection the substrate is (i.e., physical limits in terms of QE and k_{cat}/K_m). For example, DNAFs were the most recently reported fluorogenic substrates for GSTs with catalytic efficiencies reaching 10^7 for $GSTP_{1-1}$ and rate enhancements reaching 10^7−10^8.[11] By comparing DNAFs to our substrates using the bar graph approach, we can easily see that our substrates are somewhat closer to the goal of perfection, especially for $GSTA_{1-1}$ (in theory approaching a combined score of 3).

Applications. Extremely bright fluorescent molecules can be used to study single enzyme molecules and thus offer insight into enzyme behavior. Furthermore, GSTs play key roles in inflammation, pathophysiology, and tumor drug resistance. Therefore, practical fluorogenic substrates for GSTs should be extremely useful and with potential applications in many areas. First of all, it has become evident that the collective behavior of enzymes that are studied in traditional setups for steady-state and pre-steady-state kinetics cannot be taken for granted as reflecting enzyme behavior at the single molecule level.[43] No information on single enzyme molecular behavior has been gathered for GSTs; in fact, only very few enzymes have been amenable to this type of analysis. In order to achieve this, extremely stable and efficient fluorogenic substrates are needed. Our discovery that 7-amino-4-methyl-3-coumarinylacetic acid, cresyl violet, and rhodamine can be efficiently released by GSTs opens the door to study GSTs at single molecule level. Second, successful quantitation of very low levels of GST activity in cell extracts and imaging of GST activity in living cells could be very useful for identifying tumor cells that overexpress GSTs. Here the release of a fluorescent molecule (not a glutathione conjugate that is usually pumped out of cells) makes it possible to achieve fluorophore cell retention (as demonstrated for CV). Additional applications of this novel series of fluorogenic substrates include sensitive detection of hybrid proteins generated by GST fusion and their binding partners for use as a signal amplification system in biodetection.

■ CONCLUSIONS

A general strategy to synthesize strongly fluorogenic and efficient substrates applicable for most glutathione transferases

has been developed. Amino group containing fluorophores are derivatized with activated benzene sulfonamides, effectively preventing fluorescence. The enzyme reaction releases the original fluorophore, a property that allows great versatility for enzymology, biotechnology applications, and cellular imaging.

EXPERIMENTAL METHODS

Enzyme Preparation. Human $GSTA_{1-1}$, $GSTA_{2-2}$, $GSTA_{3-3}$, and $GSTA_{4-4}$ were heterologously expressed from the pET-21a (+) vector in *Escherichia coli* BL-21 DE3 cells (Novagen, Madison, WI) and purified from bacterial lysate using a HiTrap SP cation-exchange column (Amersham Biosciences) as described previously.[44] Human $GSTM_{1-1}$ and $GSTM_{2-2}$ were heterologously expressed from the pKK-D vector[45] in *E. coli* XL1-Blue cells (Strategene, La Jolla, CA) and purified by affinity chromatography as described previously.[46,47] Human $GSTP_{1-1}$ was expressed and purified as described previously.[48] Human $GSTT_{1-1}$ was expressed and purified as described previously.[49] The high purity of the enzymes was confirmed by SDS/PAGE stained with Commassie Brilliant Blue R-250. $MGST_1$ was purified from male Sprague−Dawley rat livers as described previously,[18] with the exception that 0.2% Triton X-100 was used in the last purification step. Protein concentration was determined using the method of Peterson with bovine serum albumin as standard[50] or by spectroscopic quantification (cytosolic GSTs) based on known extinction coefficients at 280 nm.

Measurement of GST Activity with Standard Substrates. The specific activity of the purified cytosolic GSTs (except $GSTT_{1-1}$) and $MGST_1$ was measured using 5 mM GSH (Sigma-Aldrich, St. Louis, MO) and 0.5 mM CDNB (Merck, Darmstadt, Germany) as second substrate in a 100 μL cuvette with a single-beam Philips PU8700 UV/visible spectrophotometer (Philips Scientific & Analytical Equipment, Cambridge, UK) by following the change in absorbance at 340 nm. The specific activity of $GSTT_{1-1}$ was determined with 0.5 mM 1,2-epoxy-3-(*p*-nitrophenoxy)propane (EPNP, Sigma-Aldrich, St. Louis, MO) instead of CDNB as second substrate by monitoring the change in absorbance at 360 nm. The molar extinction coefficients used for CDNB conjugation and EPNP conjugation were 9.6 and 0.5 $mM^{-1}cm^{-1}$, respectively.[51] All enzyme activity measurements were performed at room temperature. The cytosolic GSTs were assayed in 0.1 M potassium phosphate buffer pH 6.5, whereas $MGST_1$ was assayed in 0.1 M potassium phosphate buffer pH 6.5 containing 0.1% Triton X-100 (required for enzyme solubility, Sigma-Aldrich, St. Louis, MO). Enzymatic activities were calculated after correction for the nonenzymatic reaction. These measurements were performed in order to validate the activity and stability of the enzymes. The specific activities were in general agreement with the values reported previously.[48,52]

Novel GST Activity Assay Based on Monitoring Fluorophore Release. The conjugation of GSH with the fluorogenic probes catalyzed by cytosolic and microsomal GSTs was measured with a Shimadzu RF-510LC fluorescence spectrophotometer (Analytical Instruments Division, Kyoto, Japan) by monitoring the release of the relevant fluorophores. Essentially the same assay protocol as that described above was used with DNs-Coum, DNs-AcRh, MNs-AcRh, PBs-AcRh, DNs-CV, MNs-CV, or Ts-CV as second substrate. The concentration of DNs-Coum used was 40 μM, the concentration of DNs-AcRh, MNs-AcRh, and PBs-AcRh used was 25 μM, and the concentration of DNs-CV, MNs-CV, and Ts-CV used was 2.5 μM. Initial rates were calculated from the relative increase in fluorescence intensity when 7-amino-4-methyl-3-coumarinylacetic acid (Coum, E_x = 375 nm, E_m = 450 nm), *N*-acetylrhodamine (AcRh, E_x = 490 nm, E_m = 522 nm) or cresyl violet (CV, E_x = 540 nm, E_m = 620 nm) was formed. Calibration curves with Coum, AcRh, and CV in 0.1 M potassium phosphate buffer pH 6.5 with and without 0.1% Triton X-100 were established for quantification. Coum and CV were obtained from Sigma-Aldrich (St. Louis, MO).

Determination of Steady-State Kinetic Constants. Kinetic parameters K_m, k_{cat}, and k_{cat}/K_m for $GSTA_{1-1}$, $GSTM_{1-1}$, $GSTP_{1-1}$, and $MGST_1$ were determined with DNs-Coum, DNs-AcRh, MNs-AcRh, PBs-AcRh, and DNs-CV as substrates. The same assay conditions as those described above were used. Cytosolic GSTs ($GSTA_{1-1}$, $GSTM_{1-1}$, or $GSTP_{1-1}$) were assayed in 0.1 M potassium phosphate buffer pH 6.5, at a constant GSH concentration of 5 mM and varying concentrations of DNs-Coum (1.25−40 μM), DNs-AcRh (0.049−6.25 μM), MNs-AcRh (0.39−25 μM), PBs-AcRh (0.78−50 μM), or DNs-CV (0.1−2.5 μM), whereas $MGST_1$ was assayed in 0.1 M potassium phosphate buffer pH 6.5 containing 0.1% Triton, at a constant GSH concentration of 5 mM and varying concentrations of DNs-Coum (2.5−80 μM), DNs-AcRh (1.56−100 μM), MNs-AcRh (12.5−25 μM), PBs-AcRh (25−200 μM), or DNs-CV (0.63−20 μM). The values of the steady-state kinetic constants were determined by fitting the Michaelis−Menten equation to the data by nonlinear regression analysis using GraphPad Prism 5 (GraphPad Software, Inc., San Diego, CA). In cases where saturation was not reached, k_{cat}/K_m was determined by fitting the equation $v = (k_{cat}/K_m)[E][S]$ to the low substrate concentration data, where $K_m > [S]$. The k_{cat} value was calculated per subunit for cytosolic GSTs (25.5 kDa) and per trimer for $MGST_1$ (51 kDa for $MGST_1$), since the enzyme displays one-third of the sites reactivity.[15]

In order to assess the RE, the second-order rate constant of the nonenzymatic reaction k_{noncat} was determined and compared with the apparent second-order rate constant for the enzyme-catalyzed reaction k_{cat}/K_m (i.e., k_{cat}/K_m divided by k_{noncat}).

Cell Culture. Cell lines derived from human breast carcinoma (MCF_7 cells) were cultured as described in ref 53. In short, the $MGST_1$-expressing and vector control MCF_7 cells, which had been transfected with a vector for overexpressing rat-$MGST_1$ or the same vector containing the antisense DNA, were cultured in Dulbecco's modified Eagle's medium (DMEM, Gibco 41965), supplemented with 10% fetal bovine serum, 100 U/mL penicillin, 100 μg/mL streptomycin, 1 mM sodium pyruvate (Gibco, Paisley, UK), and 1 mg/mL Geneticin (G418, GE Healthcare, Piscataway, NJ) at 37 °C and 5% CO_2 in a humidified environment.

Activity Measurements with Cell Lysate. Cells were cultured in a T162 flask. When confluent, cells were washed with 1× phosphate-buffered saline (PBS), trypsinized, resuspended in culture medium, and centrifuged at 2000 rpm for 5 min. The medium was removed and the pellet was resuspended in 0.1 M potassium phosphate buffer pH 6.5 containing 1% Triton X-100, transferred to an Eppendorf tube, and kept on ice. Sonication was performed for 3 × 10 s at 6 A on ice with an MSE Soniprep 150 (Sanyo Gallenkamp PLC, Leicester, UK). The GST activity was then determined with the fluorogenic probes in 0.1 M potassium phosphate buffer pH 6.5 containing 0.1% Triton, using the same assay protocol as that described under "Novel GST Activity Assay Based on Monitoring Fluorophore Release". $MGST_1$ was activated by incubation of the cell suspension with 5 mM NEM (Sigma-Aldrich, St. Louis, MO) on ice for 15 min, and the reaction was terminated by the addition of 5 mM GSH. Protein concentration was determined by the Micro BCA protein assay kit (Pierce, Rockford, IL; No. 23235) in a 96-well plate with bovine serum albumin as standard.

Fluorescence Microscopic Imaging. The $MGST_1$-expressing and vector control MCF_7 cells were seeded at a density of 1×10^5 cells/well in a 6-well plate and cultured until 80−90% confluent (~48 h). Imaging experiments were then carried out. Cells were washed with 1 × PBS and incubated with one of the fluorogenic probes (DNs-Coum, DNs-AcRh, or DNs-CV) in serum-free DMEM without phenol red (Gibco 21063) (0.2% DMSO as a cosolvent) at 37 °C for 30 min. The medium was replaced with new serum-free DMEM without phenol red, and fluorescence images were captured using an inverted Nikon

ECLIPSE TE2000-S fluorescence microscope at 400× magnification. Cells were then fixed for 15 min at room temperature with 2% formaldehyde and DNA was stained with 1 μg/mL Hoechst 33342 (Invitrogen, Paisley, UK) for 10 min on shaker at room temperature to localize nuclei. Fluorescence images were captured again at 400× magnification. As a negative control, cells were pretreated with 500 μM NEM for 15 min before adding either of the fluorogenic probes.

■ ASSOCIATED CONTENT

Supporting Information. Details of probe synthesis and ^{1}H NMR and ^{13}C NMR data. This material is available free of charge via the Internet at http://pubs.acs.org.

■ AUTHOR INFORMATION

Corresponding Author
ralf.morgenstern@ki.se; h-abe@riken.jp

■ ACKNOWLEDGMENT

These studies were supported by the Swedish Research Council, Swedish Foundation for Strategic Research, VINNOVA, and funds from Karolinska Institutet. H.A. was financially supported by MEXT (Ministry of Education, Culture, Sports, Science and Technology of Japan). A.S. was financially supported by Grant-in-Aid for Young Scientists (B) (22790124) and the Special Post-doctoral Researcher Program of RIKEN. We are grateful to Dr. Koshino for NMR analysis (Molecular Characterization Team, RIKEN).

■ REFERENCES

(1) Mannervik, B.; Danielson, U. H. *CRC Crit. Rev. Biochem.* **1988**, *23*, 283.
(2) Josephy, P. D.; Mannervik, B. *Molecular Toxicology*; 2nd ed.; Oxford University Press: New York, 2006.
(3) Hayes, J. D.; Flanagan, J. U.; Jowsey, I. R. *Annu. Rev. Pharmacol. Toxicol.* **2005**, *45*, 51.
(4) McIlwain, C. C.; Townsend, D. M.; Tew, K. D. *Oncogene* **2006**, *25*, 1639.
(5) Sheehan, D.; Meade, G.; Foley, V. M.; Dowd, C. A. *Biochem. J.* **2001**, *360*, 1.
(6) Zimniak, P.; Singh, S. P. In *Toxicology of Glutathione Transferases*; Awasthi, Y. C., Ed.; CRC Press, Taylor & Francis Group, LLC: Boca Raton, FL, 2007; p 11.
(7) Morgenstern, R.; DePierre, J. W.; Ernster, L. *Biochem. Biophys. Res. Commun.* **1979**, *87*, 657.
(8) Morgenstern, R.; Meijer, J.; Depierre, J. W.; Ernster, L. *Eur. J. Biochem.* **1980**, *104*, 167.
(9) Morgenstern, R.; Svensson, R.; Bernat, B. A.; Armstrong, R. N. *Biochemistry* **2001**, *40*, 3378.
(10) Shimoji, M.; Aniya, Y.; Morgenstern, R. In *Toxicology of Glutathione Transferases*; Awasthi, Y. C., Ed.; CRC Press, Taylor & Francis Group, LLC: Boca Raton, FL, 2007; p 293.
(11) Svensson, R.; Alander, J.; Armstrong, R. N.; Morgenstern, R. *Biochemistry* **2004**, *43*, 8869.
(12) Morgenstern, R.; Guthenberg, C.; Depierre, J. W. *Eur. J. Biochem.* **1982**, *128*, 243.
(13) Morgenstern, R.; DePierre, J. W. *Eur. J. Biochem.* **1983**, *134*, 591.
(14) Weinander, R.; Ekstrom, L.; Andersson, C.; Raza, H.; Bergman, T.; Morgenstern, R. *J. Biol. Chem.* **1997**, *272*, 8871.
(15) Ricci, G.; Caccuri, A. M.; Lo Bello, M.; Pastore, A.; Piemonte, F.; Federici, G. *Anal. Biochem.* **1994**, *218*, 463.
(16) Meyer, D. J.; Coles, B.; Pemble, S. E.; Gilmore, K. S.; Fraser, G. M.; Ketterer, B. *Biochem. J.* **1991**, *274* (Pt 2), 409.
(17) Bolton, R. M.; Haritos, V. S.; Whitehouse, M. W.; Ahokas, J. T. *Anal. Biochem.* **1994**, *216*, 418.
(18) Nauen, R.; Stumpf, N. *Anal. Biochem.* **2002**, *303*, 194.
(19) Cook, J. A.; Iype, S. N.; Mitchell, J. B. *Cancer Res.* **1991**, *51*, 1606.
(20) Shrieve, D. C.; Bump, E. A.; Rice, G. C. *J. Biol. Chem.* **1988**, *263*, 14107.
(21) Rice, G. C.; Bump, E. A.; Shrieve, D. C.; Lee, W.; Kovacs, M. *Cancer Res.* **1986**, *46*, 6105.
(22) Svensson, R.; Greno, C.; Johansson, A. S.; Mannervik, B.; Morgenstern, R. *Anal. Biochem.* **2002**, *311*, 171.
(23) Fujikawa, Y.; Urano, Y.; Komatsu, T.; Hanaoka, K.; Kojima, H.; Terai, T.; Inoue, H.; Nagano, T. *J. Am. Chem. Soc.* **2008**, *130*, 14533.
(24) de Silva, A. P.; Gunaratne, H. Q.; Gunnlaugsson, T.; Huxley, A. J.; McCoy, C. P.; Rademacher, J. T.; Rice, T. E. *Chem Rev* **1997**, *97*, 1515.
(25) Uchiyama, S.; Takehira, K.; Kohtani, S.; Imai, K.; Nakagaki, R.; Tobita, S.; Santa, T. *Org. Biomol. Chem.* **2003**, *1*, 1067.
(26) Jiang, W.; Fu, Q.; Fan, H.; Ho, J.; Wang, W. *Angew. Chem., Int. Ed.* **2007**, *46*, 8445.
(27) Pu, L. *Chem. Rev.* **2004**, *104*, 1687.
(28) Koeplinger, K. A.; Zhao, Z.; Peterson, T.; Leone, J. W.; Schwende, F. S.; Heinrikson, R. L.; Tomasselli, A. G. *Drug Metab. Dispos.* **1999**, *27*, 986.
(29) Zhao, Z.; Koeplinger, K. A.; Peterson, T.; Conradi, R. A.; Burton, P. S.; Suarato, A.; Heinrikson, R. L.; Tomasselli, A. G. *Drug Metab. Dispos.* **1999**, *27*, 992.
(30) Shibata, A.; Furukawa, K.; Abe, H.; Tsuneda, S.; Ito, Y. *Bioorg. Med. Chem. Lett.* **2008**, *18*, 2246.
(31) Alander, J.; Johansson, K.; Heuser, V. D.; Farebo, H.; Jarvliden, J.; Abe, H.; Shibata, A.; Ito, M.; Ito, Y.; Morgenstern, R. *Anal. Biochem.* **2009**, *390*, 52.
(32) Shibata, A.; Abe, H.; Ito, M.; Kondo, Y.; Shimizu, S.; Aikawa, K.; Ito, Y. *Chem. Commun. (Cambridge)* **2009**, 6586.
(33) Lavis, L. D.; Chao, T. Y.; Raines, R. T. *ACS Chem. Biol.* **2006**, *1*, 252.
(34) In *Lehninger Principles of Biochemistry*, 4th ed.; Nelson, D. L., Cox, M. M., Eds.; W. H. Freeman & Co.: New York, 2004; p 190.
(35) Albery, W. J.; Knowles, J. R. *Biochemistry* **1976**, *15*, 5631.
(36) Morgenstern, R.; Lundqvist, G.; Hancock, V.; DePierre, J. W. *J. Biol. Chem.* **1988**, *263*, 6671.
(37) Paumi, C. M.; Ledford, B. G.; Smitherman, P. K.; Townsend, A. J.; Morrow, C. S. *J. Biol. Chem.* **2001**, *276*, 7952.
(38) Weinander, R.; Mosialou, E.; DeJong, J.; Tu, C. P.; Dypbukt, J.; Bergman, T.; Barnes, H. J.; Hoog, J. O.; Morgenstern, R. *Biochem. J.* **1995**, *311* (Pt 3), 861.
(39) Townsend, A. J.; Tu, C. P.; Cowan, K. H. *Mol. Pharmacol.* **1992**, *41*, 230.
(40) Morrow, C. S.; Chiu, J.; Cowan, K. H. *J. Biol. Chem.* **1992**, *267*, 10544.
(41) Morgenstern, R. *Chem. Res. Toxicol.* **1998**, *11*, 703.
(42) Rahavendran, S. V.; Karnes, H. T. *J. Pharm. Biomed. Anal.* **1996**, *15*, 83.
(43) Yang, H.; Luo, G.; Karnchanaphanurach, P.; Louie, T. M.; Rech, I.; Cova, S.; Xun, L.; Xie, X. S. *Science* **2003**, *302*, 262.
(44) Gustafsson, A.; Mannervik, B. *J. Mol. Biol.* **1999**, *288*, 787.
(45) Bjornestedt, R.; Widersten, M.; Board, P. G.; Mannervik, B. *Biochem. J.* **1992**, *282* (Pt 2), 505.
(46) Widersten, M.; Huang, M.; Mannervik, B. *Protein Expression Purif.* **1996**, *7*, 367.
(47) Johansson, A. S.; Bolton-Grob, R.; Mannervik, B. *Protein Expression Purif.* **1999**, *17*, 105.
(48) Johansson, A. S.; Stenberg, G.; Widersten, M.; Mannervik, B. *J. Mol. Biol.* **1998**, *278*, 687.
(49) Shokeer, A.; Larsson, A. K.; Mannervik, B. *Biochem. J.* **2005**, *388*, 387.

(50) Peterson, G. L. *Anal. Biochem.* **1977**, *83*, 346.
(51) Habig, W. H.; Pabst, M. J.; Jakoby, W. B. *J. Biol. Chem.* **1974**, *249*, 7130.
(52) Mannervik, B.; Widersten, M. In *Advances in Drug Metabolism in Man*; Pacifici, G. M., Fracchia, G. N., Eds.; European Commission: Luxembourg, 1995, p 407.
(53) Johansson, K.; Ahlen, K.; Rinaldi, R.; Sahlander, K.; Siritantikorn, A.; Morgenstern, R. *Carcinogenesis* **2007**, *28*, 465.